Optical Engineering

OpticalEngineering.SPIEDigitalLibrary.org

Near-infrared transmittance enhancement using fully conformal antireflective structured surfaces on microlenses fabricated by direct laser writing

Yanzeng Li
Serang Park
Daniel B. Fullager
Darrell Childers
Menelaos K. Poutous
Ishwar D. Aggarwal
Glenn Boreman
Tino Hofmann

SPIE.

Yanzeng Li, Serang Park, Daniel B. Fullager, Darrell Childers, Menelaos K. Poutous, Ishwar D. Aggarwal, Glenn Boreman, Tino Hofmann, "Near-infrared transmittance enhancement using fully conformal antireflective structured surfaces on microlenses fabricated by direct laser writing," *Opt. Eng.* **58**(1), 010501 (2019), doi: 10.1117/1.OE.58.1.010501.

Near-infrared transmittance enhancement using fully conformal antireflective structured surfaces on microlenses fabricated by direct laser writing

Yanzeng Li,[a,*] Serang Park,[a] Daniel B. Fullager,[b] Darrell Childers,[c] Menelaos K. Poutous,[a] Ishwar D. Aggarwal,[a] Glenn Boreman,[a] and Tino Hofmann[a,d]

[a]University of North Carolina at Charlotte, Department of Physics and Optical Science, Charlotte, North Carolina, United States
[b]Lasertel North America, Tucson, Arizona, United States
[c]US CONEC, Hickory, North Carolina, United States
[d]Linköping University, THz Materials Analysis Center, Department of Physics, Chemistry, and Biology (IFM), Linköping, Sweden

Abstract. Structured surfaces composed of subwavelength-sized features offer multifunctional properties including antireflective characteristics that are increasingly important for the development of micro-optical components. Here, three-dimensional (3-D) direct laser writing, via two-photon polymerization, is used to fabricate planoconvex spherical microlenses with antireflective structured surfaces. The surfaces are composed of subwavelength-sized conicoid structures, which are arranged fully conformal to the convex surface of the microlenses. The dimensions of the conicoid structures are optimized to effectively reduce Fresnel reflection loss over a wide band in the near-infrared spectral range from 1.4 to 2.2 μm, with a maximum reduction at 1.55 μm. Infrared reflection and transmission measurements are used, in combination with 3-D finite element calculations, to investigate the performance of the microlenses. The experimental results reveal that in the spectral range from 1.4 to 2.2 μm an effective suppression of the Fresnel reflection loss at the convex surface of spherical microlenses can be achieved. The transmittance enhancement is ranging from 1% to 3% for spherical microlenses with antireflective structured surfaces, in comparison to an uncoated reference. [DOI: 10.1117/1.OE.58.1.010501]

Keywords: microlens fabrication; antireflection coatings; direct laser writing; nanostructures.

Paper 181609L received Nov. 8, 2018; accepted for publication Jan. 4, 2019; published online Jan. 26, 2019.

1 Introduction

Microlenses are ubiquitous optical components with numerous applications ranging from imaging[1] and sensing,[2] to optical interconnects,[3] and even photovoltaics.[4,5] The optical performance of microlenses is impaired by Fresnel reflection losses, which are traditionally suppressed by the use of multilayered, thin-film antireflective (AR) coatings.[6–8] Fabrication requirements and properties of these multilayered, thin-film AR coatings have several inherent drawbacks, such as susceptibility to thermal deformation and stresses, limited range of suitable materials, and incident angle sensitivity, for instance.[9] These can substantially hinder the applicability of multilayered, thin-film AR coatings for microlenses, which often have a very short radius of curvature.[10,11] Single-layered AR surfaces composed of subwavelength-sized structures have been introduced more recently.[12,13] These antireflective structured surfaces (ARSSs) address some of the critical shortcomings of multilayered, thin-film AR coatings. In addition, ARSSs allow the tailoring of the index profile[14] and enable frequency-independent Fresnel reflection reduction if randomized ARSSs are used.[15] Furthermore, ARSSs can be designed to exhibit multifunctional properties, such as hydro- and oleophobic characteristics.[16,17] Moreover, ARSSs are commonly fabricated using a single material component and can be directly fabricated on lens substrate material, which can significantly simplify the fabrication process.

It is well known that the optical properties of ARSSs depend critically on its constituents' structural parameters, such as shape, height, periodic distance (pitch), volume density, and arrangement.[18] The dependence on the constituents' geometry and arrangement has been studied in detail and was optimized for planar surfaces.[19–22] Information on conformal ARSSs optimized for microlenses, however, is sparse. This is due to a lack of flexible fabrication approaches for conformal ARSSs. So far, notable works applied nanoimprint,[13,23,24] interference lithography,[12,25] or plasma etching[26–28] for the fabrication of conformal ARSSs. While providing efficient access to large-scale manufacturing, these fabrication strategies have limited capabilities for rapid prototyping and simultaneous optimization of the optical performance of the microlenses and the ARSS. In addition, ARSSs fabricated with these techniques often suffer from density variations within the ARSS across curved surfaces, rendering the ARSSs not fully conformal, thus adversely impacting their optical performance.

Three-dimensional direct laser writing (3-D DLW) might provide an attractive avenue for the fabrication of ARSSs and has been recently demonstrated by Kowalczyk et al.[21] for the first time. However, 3-D DLW-based fabrication of microlenses with conformal ARSSs has not been reported yet despite the recent success in the fabrication of bare microlenses using this technique.[29,30]

In this paper, we demonstrate a 3-D DLW-based, rapid prototyping approach for the fabrication of planoconvex spherical microlenses, with fully conformal broadband ARSSs for the near-infrared spectral range. The dimensions of the ARSS constituents are optimized for achieving maximum AR performance in the vicinity of the telecommunication wavelength of 1.55 μm. Our observations show that 3-D DLW allows for rapid fabrication and cost-effective optimization of fully conformal ARSSs, in combination with

*Address all correspondence to Yanzeng Li, E-mail: yli91@uncc.edu

0091-3286/2019/$25.00 © 2019 SPIE

microlenses designed for the infrared spectral range, when compared to previously demonstrated methods.

2 Materials and Methods

The structural features of the ARSS was optimized and then integrated into the convex surface of a simple planoconvex microlens, with a base diameter of 100 μm and a curvature of 0.01 μm^{-1}. The effective focal length of the microlens was 189 μm resulting in an f-number of 1.89 for operation at a wavelength of 1.55 μm. The microlenses and ARSSs were fabricated in a single fabrication step using 3-D DLW with one photopolymer (IP-Dip). The fabricated microlenses are investigated using FTIR reflection and transmission measurements. The absorption loss of the fabricated optical components is very small since the extinction coefficient κ of IP-Dip is vanishing ($<3 \times 10^{-5}$) in the investigated spectral range.[31,32] We observe an increase of 1% to 3% in transmittance for the microlenses investigated here. Complementary SEM and optical microscopy were used to confirm the geometry of the microlenses, and the integrity of the conformal ARSS. 3-D finite-element method (3-D FEM) reflection calculations using COMSOL were employed to evaluate and optimize the optical performance of the ARSS prior to the 3-D DLW fabrication.

The ARSS employed here is composed of conicoid subwavelength-sized structures that are arranged in hexagonal closed-packed fashion conformal to the convex surface of the microlens. The ARSS was optimized for the spectral range from 1.4 to 2.2 μm using Bruggemann effective medium homogenization by varying the parameters of the ARSS constituents (base diameter D and height H of the conicoids and their lateral separation P, see inset of Fig. 1) as described in detail in our previous work.[19] Note that the dielectric function of IP-Dip used for these calculations was obtained by variable angle IR ellipsometry and is reported elsewhere.[31]

For an ARSS composed of IP-Dip conicoid subwavelength-sized structures, the lowest reflectance for the spectral range from 1.4 to 2.2 μm is obtained at $\lambda = 1.55$ μm for $P = 0.9$ μm, $D = 0.8$ μm, and $H = 0.83$ μm, compared the reflectance of a planar IP-Dip surface that is 5.1%. Note that the fully conformal arrangement of the ARSSs designed and fabricated here results in conicoid structures normal to the convex surface of the microlens while preserving a constant lateral separation. Thus, simple planar surface models are suitable for the analytical and numerical evaluation of the optimal performance of the ARSS-coated microlenses.

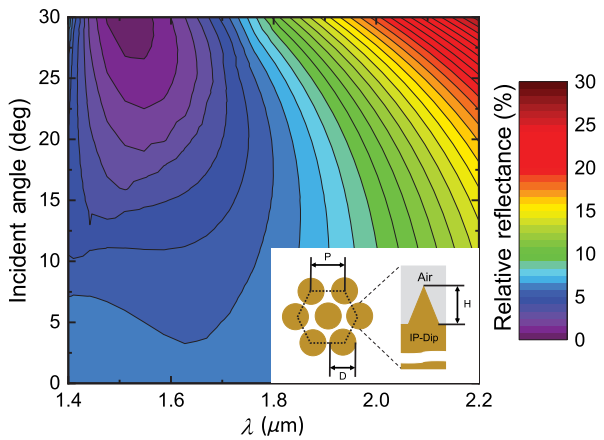

Fig. 1 Contour plot of relative specular reflectance obtained using 3-D FEM calculations, as a function of angle of incidence ranging from 0 deg to 30 deg, for the spectral range from 1.4 to 2.2 μm. The geometry of the ARSS is shown in the inset. A lateral spacing $P = 0.9$ μm, cone diameter $D = 0.8$ μm, and cone height $H = 0.83$ μm was used for the calculations. The complex dielectric properties for IP-Dip were obtained from variable angle spectroscopic ellipsometry measurements.[31] Note that the reflectance of IP-Dip over the corresponding incident angles was used as a reference.

3 Results and Discussion

Figure 1 depicts 3-D FEM-calculated relative reflectance data for an IP-Dip ARSS, which were obtained using the reflection spectra ratio of the IP-Dip ARSS to a planar IP-Dip substrate, over a spectral range from 1.4 to 2.2 μm as a function of the angle of incidence. The range of the incident angle from 0 deg to 30 deg is determined by considering the optical configuration of the Cassegrain objective used for the reflectance measurements and the variation of surface normal across the measured area of the microlens. A decrease in relative reflection of at least 30% is observed over the entire spectral and angle of incidence range of interest. In the vicinity of the telecommunication wavelength $\lambda = 1.55$ μm, the ARSS is most effective as expected based on the optimization described in Ref. 19. A minimum in the relative reflectance occurs for incidence angles >20 deg, where the calculated relative reflectance is as low as 0.2%.

3-D renderings of the microlenses with and without the ARSS coating are shown in Figs. 2(a) and 2(b), respectively. The inset of Fig. 2(b) shows a closeup of the 3-D rendering of ARSS-coated microlens to provide structural details of the AR constituents, which are homogeneously and conformally

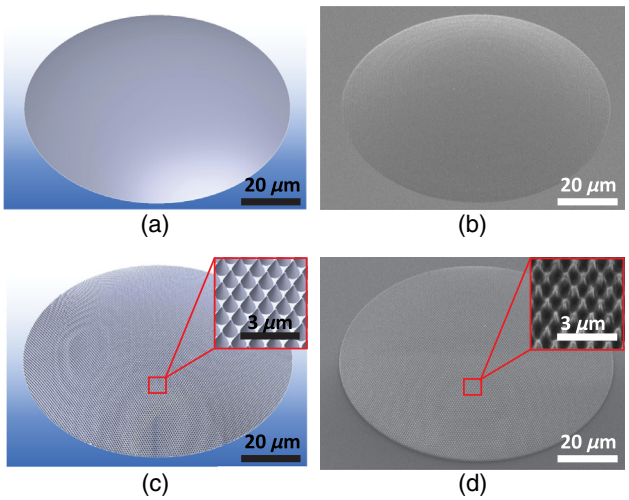

Fig. 2 3-D rendering of the nominal design of a bare planoconvex spherical microlens and a corresponding microlens with an ARSS is shown in (a) and (b), respectively. Both microlenses have a base diameter 100 μm. The inset in panel (b) depicts a closeup of the 3-D rendering of the ARSS showing the hexagonal lattice pattern of the conicoid ARSS constituents. Corresponding SEM micrographs of the fabricated bare microlens and the microlens with the conformal ARSS on the convex side are depicted in (c) and (d), respectively. The inset in panel (d) shows a closeup of the ARSS on the microlens. 3-D renderings and micrographs were obtained with a 45-deg tilt with respect to the surface normal.

distributed in a hexagonal lattice pattern across the convex lens surface.

Two planoconvex microlenses were fabricated by polymerizing IP-dip monomer on glass substrates using a commercially available 3-D DLW system (Photonic Professional GT, Nanoscribe, GmbH). One microlens was fabricated with an ARSS conformal to the convex surface while the other microlens was fabricated with a bare convex surface to serve as a reference. Both microlenses were fabricated in a single 3-D DLW fabrication step using identical exposure doses, which were optimized prior to the synthesis. After fabrication, the unpolymerized monomer is removed by immersion in propylene glycol monomethyl ether acetate (PGMEA, Baker 220), and subsequently in 99.99% isopropyl alcohol for 20 and 2 min, respectively. Finally, the remaining isopropyl alcohol is evaporated by blow-drying with dry nitrogen.

The AR performance was evaluated using FTIR reflection and transmission measurements. In addition, scanning electron microscopy (SEM) was used to determine the conformality and structural quality of the fabricated ARSS on top of the microlenses, and complementary optical microscopy was employed to evaluate the curvature of the fabricated microlenses.

Figures 2(c) and 2(d) show SEM micrographs of the fabricated bare and the ARSS-coated microlens, respectively. It can be clearly seen that the ARSS conformally follows the convex surface of the microlens. Comparing the insets of Figs. 2(b) and 2(d), a true-to-form geometry and hexagonal surface arrangement of the fabricated conicoid constituents of the ARSS can be observed.

With optical microscopy, the evaluation of the fabricated microlenses' curvature was carried out via an experimental verification of the corresponding effective focal length under white light illumination. The experimentally determined effective focal length is 175 ± 5 μm for both microlenses, consistent with the nominal effective focal length of 180 μm given by the lens curvature (0.01 μm^{-1}) and the refractive index of IP-dip ($n = 1.55$) for visible light illumination.[33]

The optical performance of the microlenses was investigated by reflection and transmission IR microscopy measurements in spectral range from 1.4 to 2.2 μm using an FTIR spectrometer in conjunction with an IR microscope (VERTEX 70 and HYPERION 3000, Bruker, Inc.). A 15× Cassegrain objective is used for the reflection measurements, whereas the transmission measurements used a complementary 15× Cassegrain condensor. The Cassegrain illumination configuration results in a range of angles of incidence from 10.8 deg to 23.5 deg defined by the numerical aperture of the Cassegrain objectives and the diameter of their central mirrors.[34]

Figure 3 depicts the experimental data for the relative reflectance (blue-solid line) and transmittance (red-solid line) spectra of the microlens with the conformal ARSS. Note that the absolute reflectance and transmittance of the bare microlens was used as a reference. On average, a 2% increase in relative transmission is observed across the investigated spectral range due to the conformal ARSS treatment of the convex microlens surface. This is in good agreement with the observed 40% reduction in relative reflectance indicating negligible absorption and scattering losses.

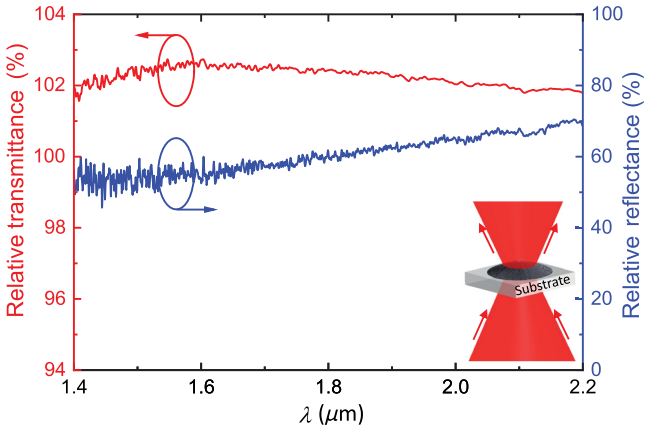

Fig. 3 Relative reflectance (blue-solid line, bottom) and transmittance (red-solid line, top) spectra of the ARSS-treated microlens [Figs. 2(b) and 2(d)] measured by FTIR microscopy in the range from 1.4 to 2.2 μm using the absolute reflectance and transmittance of a bare microlens shown in Figs. 2(a) and 2(c) as a reference, respectively. The microlenses were mounted such that convex surface of the microlens faced the Cassegrain objective as shown in the inset.

4 Conclusions

We demonstrated that 3-D DLW is an effective method for the fabrication of microlenses including conformal functional coatings for the near-infrared spectral range. Here, an ARSS composed of subwavelength-sized conicoid structures was optimized for the near-infrared spectral range and effectively used to reduce the Fresnel reflection loss at the convex surface of planoconvex spherical microlenses. A structural comparison between the nominal and as-fabricated microlenses shows a good agreement on both micron- and submicron-sized structural features and illustrates the effectiveness of 3-D DLW as a rapid prototyping tool for fabricating optical components including functional coatings with multiscale features in a single fabrication step.

Our experimental reflectance and transmittance spectra obtained using FTIR microscopy found a 2% improvement in transmission and a 40% reduction in reflection over the spectral range from 1.4 to 2.2 μm. These results are in good agreement with 3-D FEM calculations, which corroborated the experimentally observed reflectance minimum at 1.55 μm. Optical imaging was used to demonstrate the functionality of the microlenses with and without ARSS coating and verify the focal length of the microlenses. We find that 3-D DLW could offer an elegant avenue for the rapid prototyping of optical components including conformal functional coatings for the infrared spectral range.

Acknowledgments

The authors are grateful for support from the National Science Foundation (1624572) within the I/UCRC Center for Metamaterials, the Swedish Agency for Innovation Systems (2014-04712), and Department of Physics and Optical Science of the University of North Carolina at Charlotte.

References

1. J. Arai, H. Kawai, and F. Okano, "Microlens arrays for integral imaging system," *Appl. Opt.* **45**(36), 9066–9078 (2006).
2. M. Vekshin et al., "Glass microlens arrays for Shack–Hartmann wavefront sensors," *Meas. Sci. Technol.* **21**(5), 054010 (2010).

3. C. A. Edwards, H. M. Presby, and C. Dragone, "Ideal microlenses for laser to fiber coupling," *J. Lightwave Technol.* **11**(2), 252–257 (1993).
4. J. H. Karp, E. J. Tremblay, and J. E. Ford, "Planar micro-optic solar concentrator," *Opt. Express* **18**(2), 1122–1133 (2010).
5. T. Hou et al., "Fabrication, characterization, and applications of microlenses," *Appl. Opt.* **54**(24), 7366–7376 (2015).
6. E. Pawlowski et al., "Diffractive microlenses with antireflection coatings fabricated by thin film deposition," *Opt. Eng.* **33**(2), 647–653 (1994).
7. U. Schulz, "Review of modern techniques to generate antireflective properties on thermoplastic polymers," *Appl. Opt.* **45**(7), 1608–1618 (2006).
8. P. Schnauber et al., "Bright single-photon sources based on anti-reflection coated deterministic quantum dot microlenses," *Technologies* **4**(1), 1 (2015).
9. S. S. Oh, C.-G. Choi, and Y.-S. Kim, "Fabrication of micro-lens arrays with moth-eye antireflective nanostructures using thermal imprinting process," *Microelectron. Eng.* **87**(11), 2328–2331 (2010).
10. J.-Q. Xi et al., "Optical thin-film materials with low refractive index for broadband elimination of fresnel reflection," *Nat. Photonics* **1**(3), 176–179 (2007).
11. U. Schulz, "Broadband antireflection coatings for optical lenses," *SPIE Newsroom* 2–4 (2015).
12. B. Päivänranta et al., "Antireflective nanostructured microlenses," *Microelectron. Eng.* **85**(5–6), 1089–1091 (2008).
13. J.-T. Wu, W.-Y. Chang, and S.-Y. Yang, "Fabrication of a nano/micro hybrid lens using gas-assisted hot embossing with an anodic aluminum oxide (aao) template," *J. Micromech. Microeng.* **20**(7), 075023 (2010).
14. W. H. Southwell, "Gradient-index antireflection coatings," *Opt. Lett.* **8**(11), 584–586 (1983).
15. L. E. Busse et al., "Anti-reflective surface structures for spinel ceramics and fused silica windows, lenses and optical fibers," *Opt. Mater. Express* **4**(12), 2504–2515 (2014).
16. L. Peng et al., "Continuous fabrication of multiscale compound eyes arrays with antireflection and hydrophobic properties," *IEEE Trans. Nanotechnol.* **15**(6), 971–976 (2016).
17. A. Cavalli, P. Bøggild, and F. Okkels, "Parametric optimization of inverse trapezoid oleophobic surfaces," *Langmuir* **28**(50), 17545–17551 (2012).
18. D. Stavenga et al., "Light on the moth-eye corneal nipple array of butterflies," *Proc. Biol. Sci.* **273**(1587), 661–667 (2006).
19. Y. Li et al., "Broadband near-infrared antireflection coatings fabricated by three-dimensional direct laser writing," *Opt. Lett.* **43**(2), 239–242 (2018).
20. R. Weiblen et al., "Optimized moth-eye anti-reflective structures for as 2 s 3 chalcogenide optical fibers," *Opt. Express* **24**(10), 10172–10187 (2016).
21. M. Kowalczyk, J. Haberko, and P. Wasylczyk, "Microstructured gradient-index antireflective coating fabricated on a fiber tip with direct laser writing," *Opt. Express* **22**(10), 12545–12550 (2014).
22. S. Ji et al., "Optimal moth eye nanostructure array on transparent glass towards broadband antireflection," *ACS Appl. Mater. Interfaces* **5**(21), 10731–10737 (2013).
23. Y.-P. Chen, C.-H. Lee, and L. A. Wang, "Fabrication and characterization of multi-scale microlens arrays with anti-reflection and diffusion properties," *Nanotechnology* **22**(21), 215303 (2011).
24. H. K. Raut et al., "Multiscale ommatidial arrays with broadband and omnidirectional antireflection and antifogging properties by sacrificial layer mediated nanoimprinting," *ACS Nano* **9**(2), 1305–1314 (2015).
25. P.-Y. Baroni et al., "Nanostructured surface fabricated by laser interference lithography to attenuate the reflectivity of microlens arrays," *J. Eur. Opt. Soc-Rapid* **5**, 10006 (2010).
26. J. W. Leem, Y. M. Song, and J. S. Yu, "Biomimetic artificial si compound eye surface structures with broadband and wide-angle antireflection properties for si-based optoelectronic applications," *Nanoscale* **5**(21), 10455–10460 (2013).
27. H. Jung and K.-H. Jeong, "Monolithic polymer microlens arrays with antireflective nanostructures," *Appl. Phys. Lett.* **101**(20), 203102 (2012).
28. Y. M. Song et al., "Multifunctional light escaping architecture inspired by compound eye surface structures: from understanding to experimental demonstration," *Opt. Express* **19**(102), A157–A165 (2011).
29. T. Gissibl et al., "Two-photon direct laser writing of ultracompact multi-lens objectives," *Nat. Photonics* **10**(8), 554–560 (2016).
30. N. Tsutsumi et al., "Direct laser writing for micro-optical devices using a negative photoresist," *Opt. Express* **25**(25), 31539–31551 (2017).
31. D. B. Fullager, G. D. Boreman, and T. Hofmann, "Infrared dielectric response of nanoscribe ip-dip and ip-l monomers after polymerization from 250 cm^{-1} to 6000 cm^{-1}," *Opt. Mater. Express* **7**(3), 888–894 (2017).
32. S. Dottermusch et al., "Exposure-dependent refractive index of nanoscribe ip-dip photoresist layers," *Opt. Lett.* **44**(1), 29–32 (2019).
33. T. Gissibl et al., "Refractive index measurements of photo-resists for three-dimensional direct laser writing," *Opt. Mater. Express* **7**(7), 2293–2298 (2017).
34. K. Hinrichs et al., "Polarization-dependent and ellipsometric infrared microscopy for analysis of anisotropic thin films," *J. Phys. Chem. C* **117**(26), 13557–13563 (2013).